Cross-comparison of the IRS-P6 AWiFS sensor with the L5 TM, L7 ETM+, & Terra MODIS sensors

JACIE Workshop

March 16-18, 2010

Gyanesh Chander (gchander@usgs.gov)

SGT, Inc*., contractor to the USGS EROS, Sioux Falls, SD, 57198 USA

***Work performed under USGS contract 08HQCN0005**

U.S. Department of the Interior

U.S. Geological Survey

ResourceSat-1 (IRS-P6) Overview

- The IRS-P6 satellite was launched into a polar sun-synchronous orbit on Oct. 17, 2003, with a design life of 5 years
- IRS-P6 carries three sensors
  - **High Resolution Linear Imaging Self-Scanner (LISS-IV)**
  - **Medium Resolution Linear Imaging Self-Scanner (LISS-III)**
  - **Advanced Wide Field Sensor (AWiFS)**
- All three sensors are “Pushbroom” scanners using linear arrays of CCDs
- IRS-P6 also carries an onboard SSR with a capacity of 120 GB

IRS-P6 Orbit and Coverage Details	
Orbit Altitude	817 km
Orbit Inclination	98.69 deg
Orbit period	101.35 min
Number of Orbits per day	14.2083
Equatorial crosing time	10.30 a.m.
Repeat Cycle (LISS-III)	24 days
Repeat Cycle (LISS-IV)	5 days
Distance between adjacent paths	117.5 km
Distance between successive ground tracks	2,820 km
Lift-off Mass	1360 kg
Ground trace velocity	6.65 km/sec
Orbits/cycle	341
Semimajor axis	7195.11
Eccentricity	0.001
Mission Life	5 years

IRS-P6 Sesnsor Specifications			
	LISS-IV	LISS-III	AWiFS
Resolution (m)	5.8	23.5	56
Swath (km)	23.9 km (Mx)	141km	740 km
Spectral Bands (µm)	B2: 0.52-0.59	B2: 0.52-0.59	B2: 0.52-0.59
	B3: 0.62-0.68	B3: 0.62-0.68	B3: 0.62-0.68
	B4: 0.77-0.86	B4: 0.77-0.86	B4: 0.77-0.86
		B5: 1.55-1.70	B5: 1.55-1.70
Quantization (bits)	7	7	10
Repeat Cycle (days)	5	24	5
Integration Time (msec)	0.877714	3.32	9.96
No. of gains	Single gain	Four for B2,3,4	Single gain
Sensor	Pushbroom	Pushbroom	Pushbroom
CCD Arrays	1 * 12288	1 * 6000	2 * 6000
CCD Size (µm)	7 µm x 7 µm	10 µm x 7 µm	10 µm x 7 µm
Focal Length (mm)	982	347.5	139.5
Cross-track FOV for pixel (radiance)	0.0000071	0.0000288	0.0000717
Power (W)	216	70	114
Weight (kg)	169.5	106.1	103.6
Data Rate (MBPS)	105	52.5	52.5

G. Chander (gchander@usgs.gov) JACIE Workshop

AWiFS Sensor Collection Mode

The AWiFS camera is split into two separate electro-optic modules (AWiFS-A and AWiFS-B) tilted by 11.94 degrees with respect to nadir

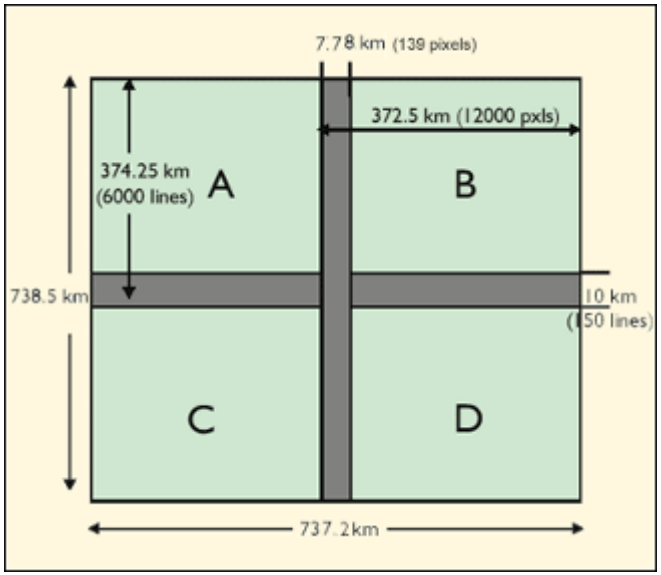

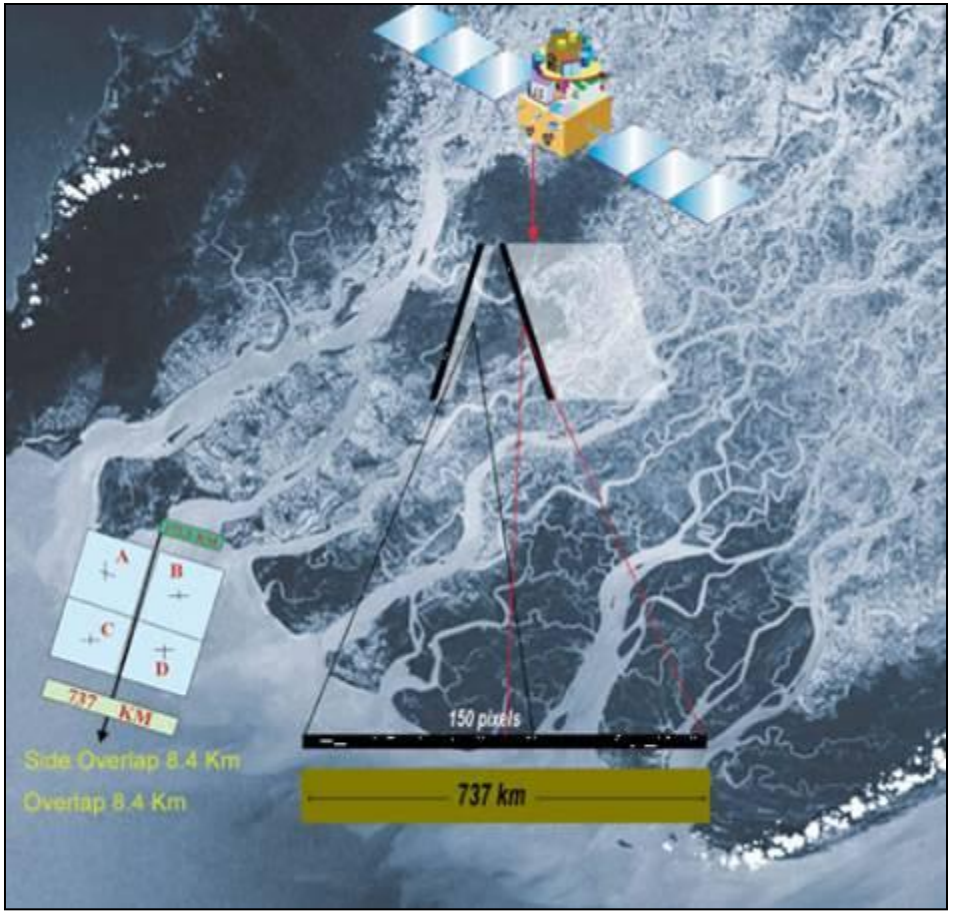

G. Chander (gchander@usgs.gov) JACIE Workshop

Sensor Overview

Platform	Landsat 5	Landsat 7	Terra	IRS-P6
Sensor	TM	ETM+	MODIS	AWiFS
Number of bands	7	8	36	4
Spatial resolution	30 m, 120 m	15 m, 30 m, 60 m	250 m, 500 m, 1 km	56 m (nadir), 70 m (edge)
Swath	183 km	183 km	2330 km	740 km
Spectral coverage	0.4~12.5 µm	0.4~12.5 µm	0.4~14 µm	0.52~1.7 µm
Pixel quantization	8 bit	8 bit	12 bit	10 bit
Launch date	1-Mar-84	15-Apr-99	18-Dec-99	17-Oct-03
Orbit type	Sun synchronous	Sun synchronous	Sun synchronous	Sun synchronous
Equatorial Crossing Time	10:00 AM	10:00 AM	10:30 AM	10:30 AM
Altitude	705 km	705 km	705 km	817 km

AWiFS VITAL FACTS:

- **Instrument: Pushbroom**
- **Bands (4): 0.52-0.59, 0.62-0.68, 0.77-0.86, 1.55-1.70 µm**
- **Spatial Resolution: 56 m (near nadir), 70 m (near edge)**
- **Radiometric Resolution: 10 bit**
- **Swath: 740 km**
- **Repeat Time: 5 days**
- **Design Life: 5 years**

G. Chander (gchander@usgs.gov) JACIE Workshop

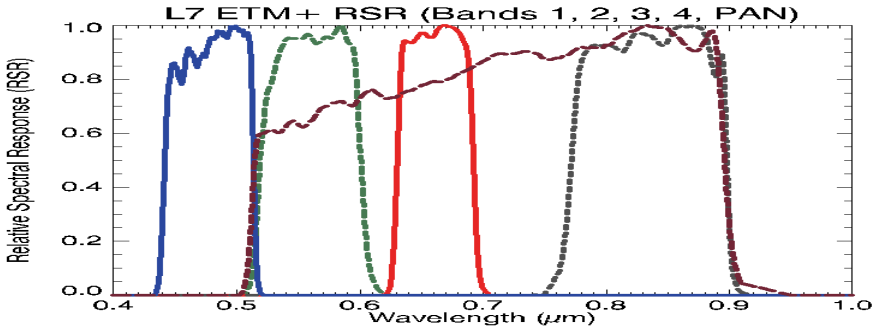
L7 ETM+ RSR (Bands 1, 2, 3, 4, PAN)
Relative Spectral Response (RSR)
Wavelength (μm)

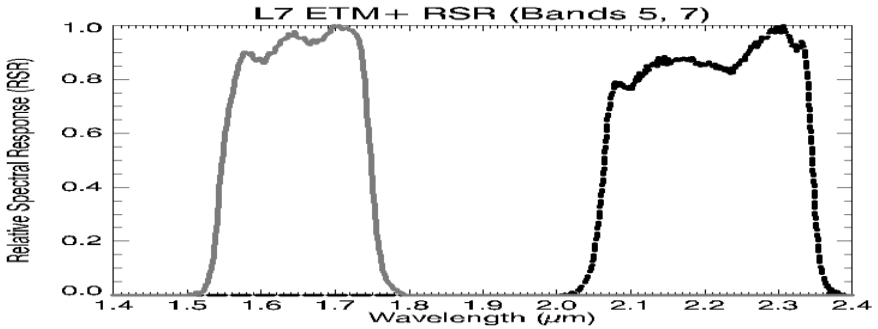
L7 ETM+ RSR (Bands 5, 7)
Relative Spectral Response (RSR)
Wavelength (μm)

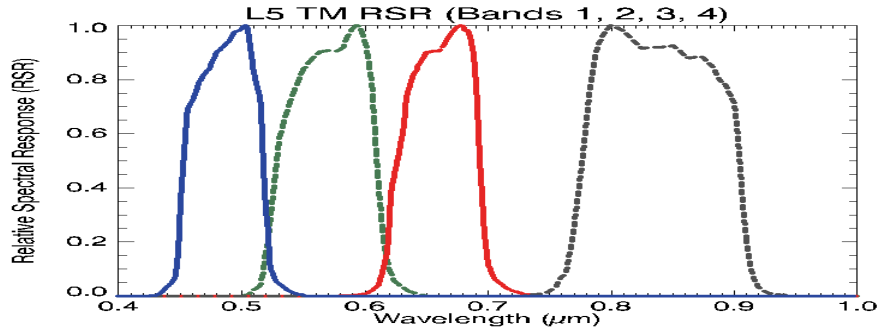
L5 TM RSR (Bands 1, 2, 3, 4)
Relative Spectral Response (RSR)
Wavelength (μm)

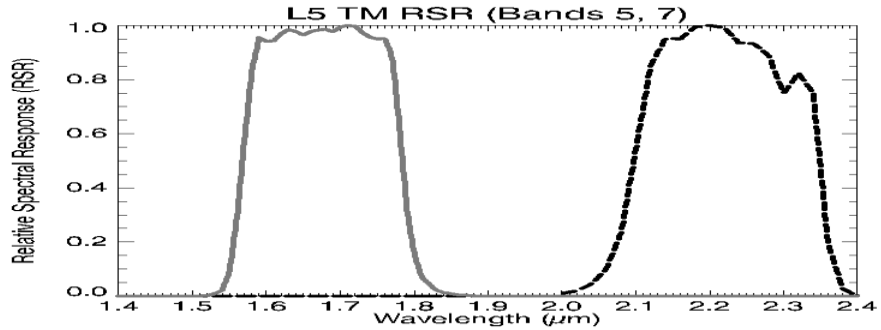
L5 TM RSR (Bands 5, 7)
Relative Spectral Response (RSR)
Wavelength (μm)

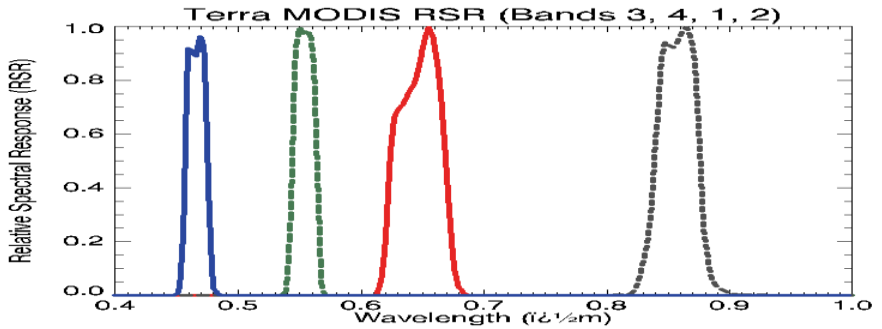
Terra MODIS RSR (Bands 3, 4, 1, 2)
Relative Spectral Response (RSR)
Wavelength (ï¿½m)

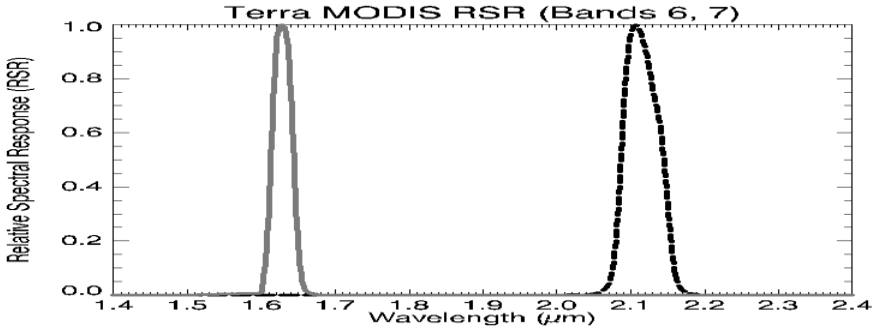
Terra MODIS RSR (Bands 6, 7)
Relative Spectral Response (RSR)
Wavelength (μm)

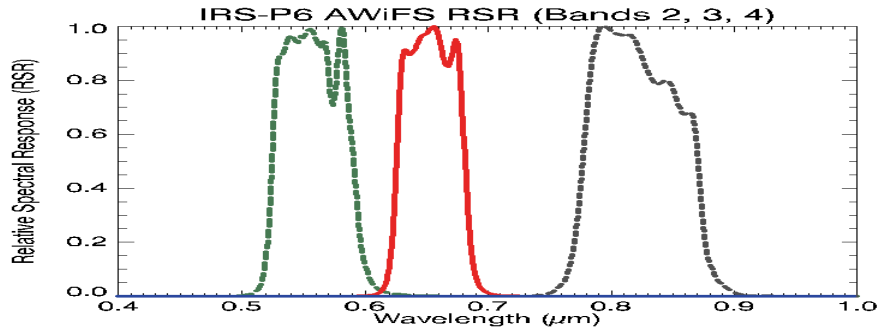
IRS-P6 AWiFS RSR (Bands 2, 3, 4)
Relative Spectral Response (RSR)
Wavelength (μm)

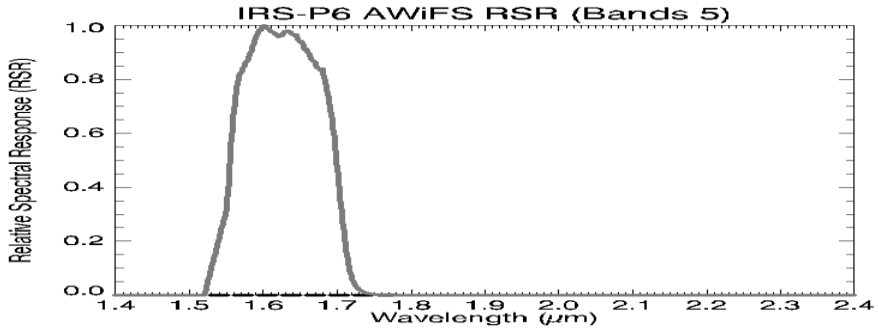
IRS-P6 AWiFS RSR (Bands 5)
Relative Spectral Response (RSR)
Wavelength (μm)

AWiFS Data Products

	Standard Products	Value Added Products
1	Path/Row Based	Precision Geocoded Products
2	Shift Along Track Product	Template registered products
3	Quadrant Products	Merge Products
4	Georeferenced Products	Ortho products
5	Geocoded Products	
6	Basic Stereo Pair	

Level	Type of Correction
Level-0	No correction (Raw)
Level-1	Radiometric correction
Level-2	Radiometric and Geometric correction (Standard)
Level-3	Precision correction using GCPs

Resampling Options	Map Projections	Earth Ellipsoids	Digital Data Product formats
Cubic Convolution (C)	Polyconic (P)	Clarke 1866 (C6)	LGSOWG Superstructure Format
Nearest Neighbour (N)	Lambert Conformal Conical (L)	International 1909 (I9)	Fast Format
Bilinear (B)	Universal Transverse Mercator (U)	GRS 1980 (GR)	GeoTiff-Gray Scale
16 Point Sinc (S)	Space Oblique Mercator (S)	Everest (EV)	GeoTiff-RGB
Kaiser-16 (K)		WGS – 84 (W4)	HDF
4 Point Sinc (F)		Bessel (BL)	
		Krassovsky (KW)	

- Space Imaging (now GeoEye) was granted a license to receive & distribute AWiFS imagery from their ground station in Oklahoma (Jan. 2005)
- Effective 1 January 2009, EOTec became the exclusive distributors for Resourcesat Data in North America (GeoEye is key partner)

USDA Satellite Imagery Archive

The USDA AWiFS imagery product was standardized using the following parameters

1. Item: AWiFS orthorectified quad. L1T (terrain-corrected)
2. Identification: path, row, quad, date
3. Projection: Lambert Conformal Conic
4. Resampling: Cubic convolution
5. Datum: WGS84
6. Orientation: North up
7. Format: 4-bands, unstacked geoTIFF
8. Bit depth: 8-bits (**10 bits for data processed after 4/1/2008**)
9. Media: CDROM
10. License for redistribution: Tier 2 (Federal/Civilian agencies)

G. Chander (gchander@usgs.gov) JACIE Workshop

AWiFS Data Holding in USDA

- 2004 to 2010 data available in the USDA Archive Explorer v.3.1 (**6,314** AWiFS scenes)
- 2004 to 2007 data available in EE (**2,922** scenes)

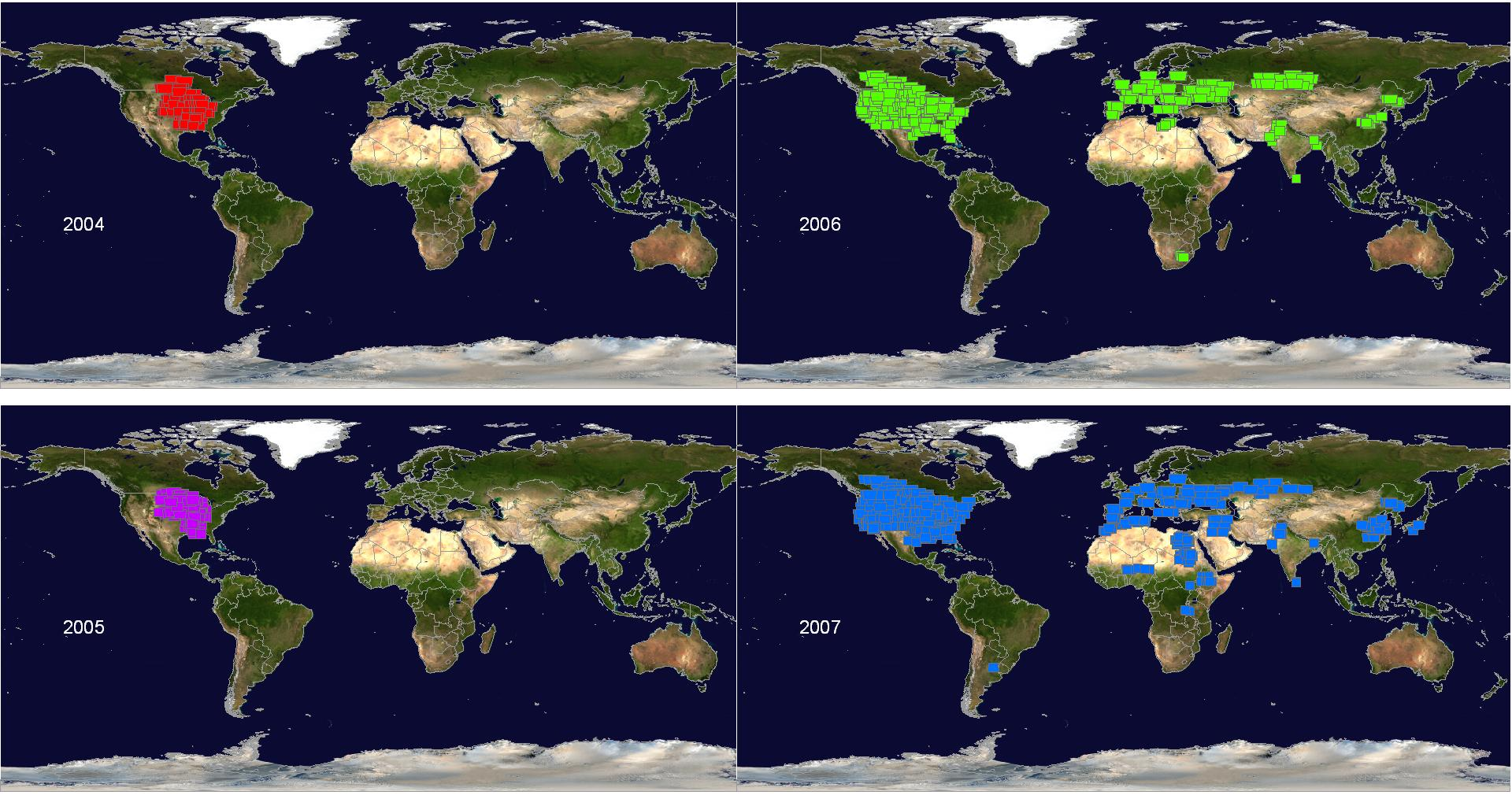

Conversion to Radiance (IRS-P6 data)

$$L_{rad} = \frac{(L_{\max} - L_{\min})}{Q_{cal\,\max}} \cdot Q_{cal} + L_{\min}$$

Where

- **L* = spectral radiance at the sensor's aperture**
- **Qcal = Calibrated Digital Number**
- **Qcalmax = maximum possible DN value**
  - 255 for LISS-IV & LISS-III products
  - 1023 for 10-bit AWiFS
  - 255 for 8-bit AWiFS products
- **Lmax & Lmin = scaled spectral radiance (provided in the header file)**
  - For GeoTIFF products, these values are found in the Image Description field of the GeoTIFF header
  - For Fast Format products, values are in the HEADER.DAT
  - For LGSOWG products, values are in the leader file

Ortho Generation 10-to-8 bit rescaling

$$L_{rad} = \frac{DN_{10}}{1023} \cdot (L_{\max} - L_{\min}) + L_{\min}$$

$$DN_8 = DN_{10} \cdot \frac{255}{1023}$$

$$L_{rad} = \frac{DN_8}{255} \cdot (L_{\max} - L_{\min}) + L_{\min}$$

G. Chander (gchander@usgs.gov) JACIE Workshop

Header File Information (Lmax & Lmin)

LISS-IV Mono Band 3:
Onboard gain number for band 3 3
Minimum / maximum radiance for band 3 [mw/cm2/str/um] ... 0.00000 9.92230

LISS-III:
Onboard gain number for band 2 3
Onboard gain number for band 3 3
Onboard gain number for band 4 3
Onboard gain number for band 5 2
Minimum / maximum radiance for band 2 [mw/cm2/str/um] ... 0.00000 12.06400
Minimum / maximum radiance for band 3 [mw/cm2/str/um] ... 0.00000 15.13100
Minimum / maximum radiance for band 4 [mw/cm2/str/um] ... 0.00000 15.75700
Minimum / maximum radiance for band 5 [mw/cm2/str/um] ... 0.00000 3.39700

AWiFS-A camera (A&C quadrant scenes):
Onboard gain number for band 2 8
Onboard gain number for band 3 9
Onboard gain number for band 4 8
Onboard gain number for band 5 9
Minimum / maximum radiance for band 2 [mw/cm2/str/um] ... 0.00000 52.34000
Minimum / maximum radiance for band 3 [mw/cm2/str/um] ... 0.00000 40.75000
Minimum / maximum radiance for band 4 [mw/cm2/str/um] ... 0.00000 28.42500
Minimum / maximum radiance for band 5 [mw/cm2/str/um] ... 0.00000 4.64500

AWiFS-B camera (B&D quadrant scenes):
Onboard gain number for band 2 8
Onboard gain number for band 3 9
Onboard gain number for band 4 8
Onboard gain number for band 5 9
Minimum / maximum radiance for band 2 [mw/cm2/str/um] ... 0.00000 52.34000
Minimum / maximum radiance for band 3 [mw/cm2/str/um] ... 0.00000 40.75000
Minimum / maximum radiance for band 4 [mw/cm2/str/um] ... 0.00000 28.42500
Minimum / maximum radiance for band 5 [mw/cm2/str/um] ... 0.00000 4.64500

Conversion to TOA Reflectance

$$\rho_\lambda = \frac{\pi \cdot L_\lambda \cdot d^2}{ESUN_\lambda \cdot \cos\theta_s}$$

ESUN values using the Thuillier solar spectrum (UNITS = W/m² μm)

Bands	L5 TM	L7 ETM+	P6 AWiFS
2	**1796**	**1812**	**1820**
3	**1536**	**1533**	**1579**
4	**1031**	**1039**	**1105**
5	**220.0**	**230.8**	**240.6**

G. Chander (gchander@usgs.gov) JACIE Workshop

L5 TM, L7 ETM+ & P6 AWiFS Image Pairs

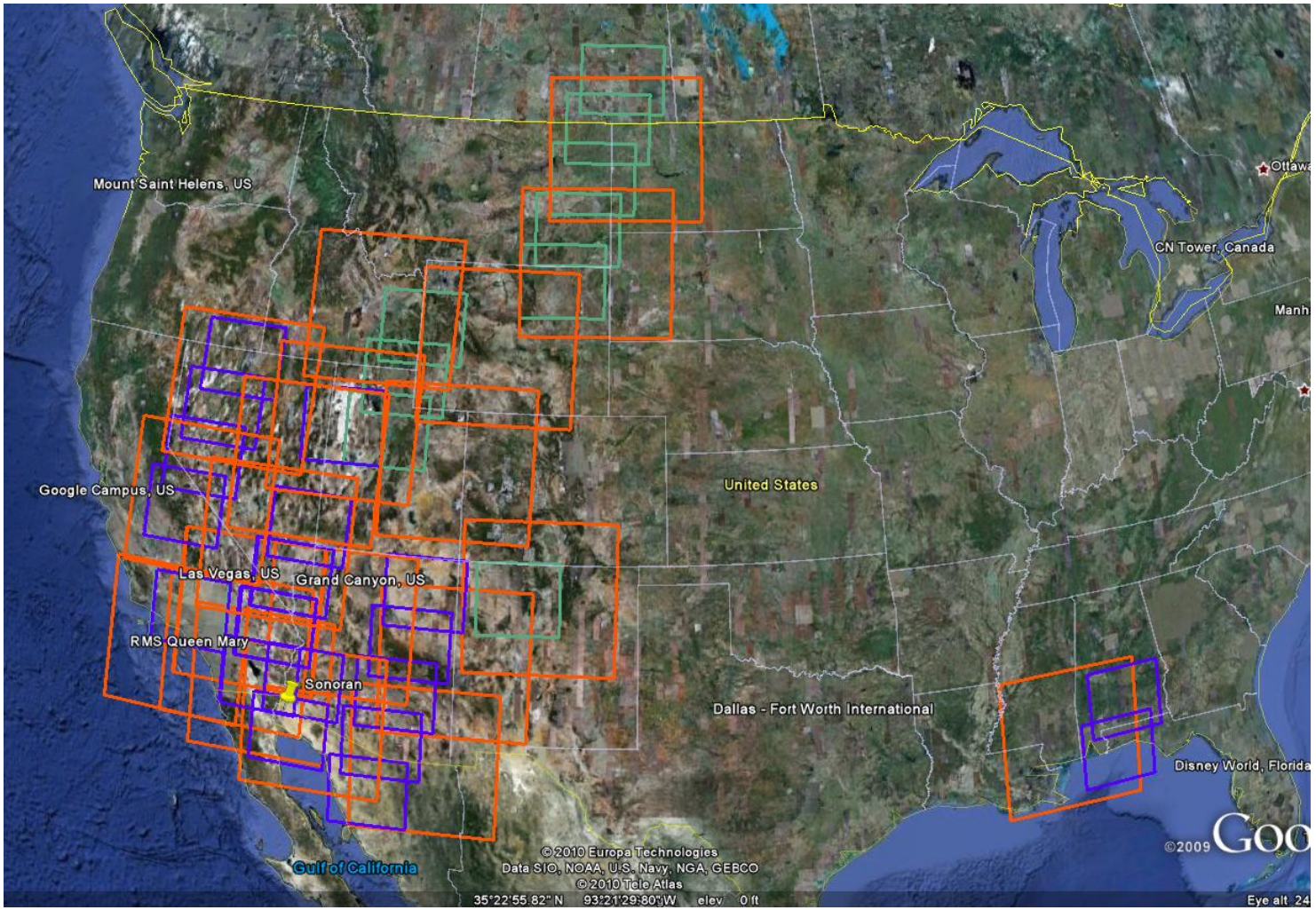

G. Chander (gchander@usgs.gov) JACIE Workshop

AWiFS cross-cal with TM, ETM+, MODIS

AWiFS versus TM

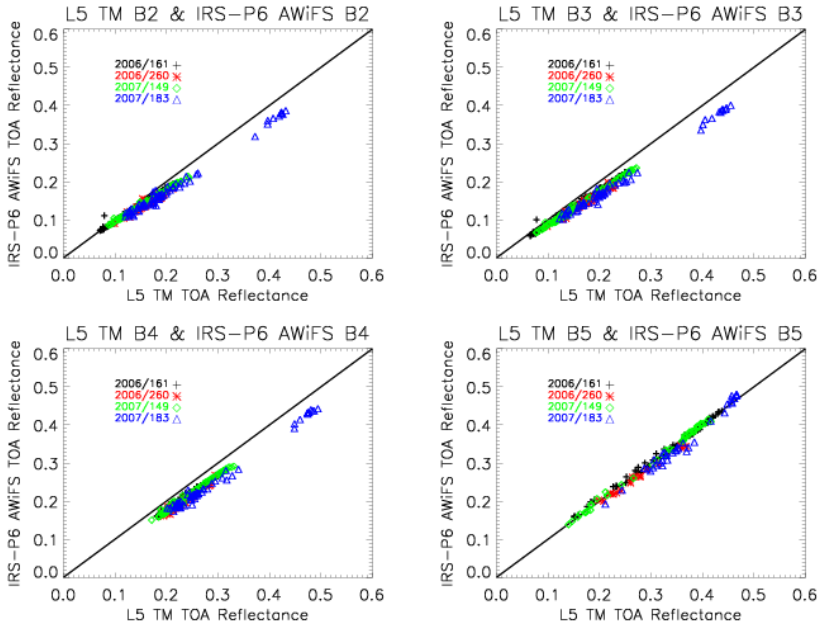

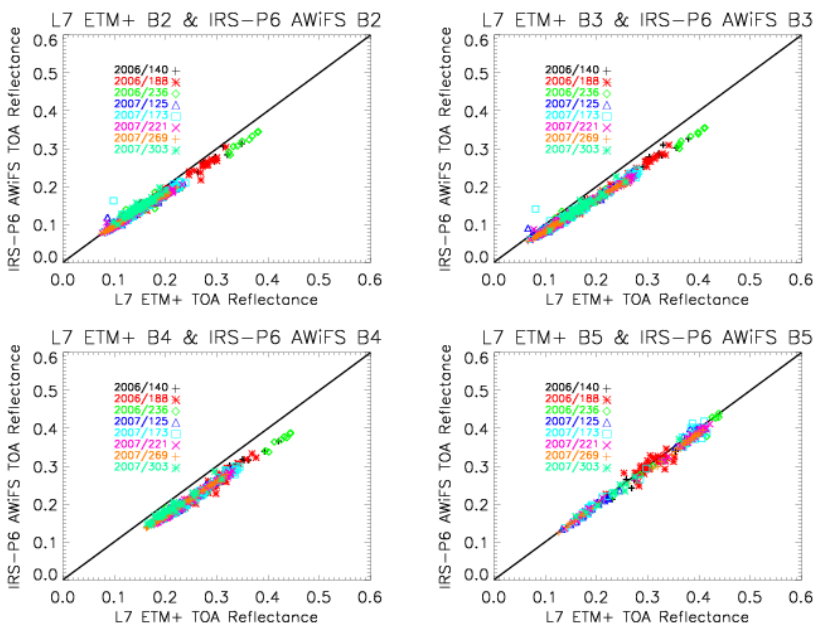

AWiFS versus ETM+

AWiFS versus MODIS

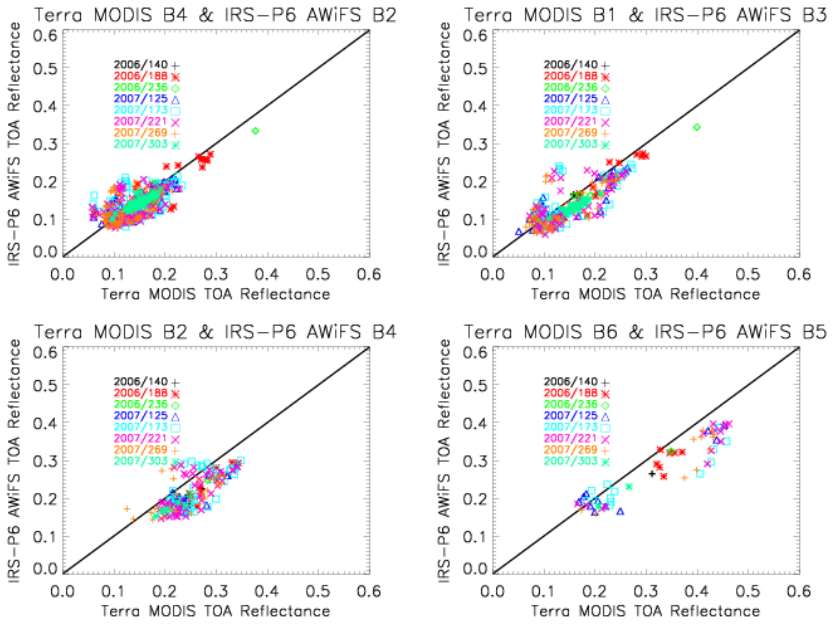

The cross-cal was performed using image statistics from large common areas observed by co-incident image pairs from the two sensors

The results indicate that the IRS-P6 AWiFS sensors can be cross-calibrated to the L5 TM sensor within an accuracy of 13%; L7 ETM+ within 14%; Terra MODIS within 23%

AWiFS Camera AC/BD cross-cal with TM

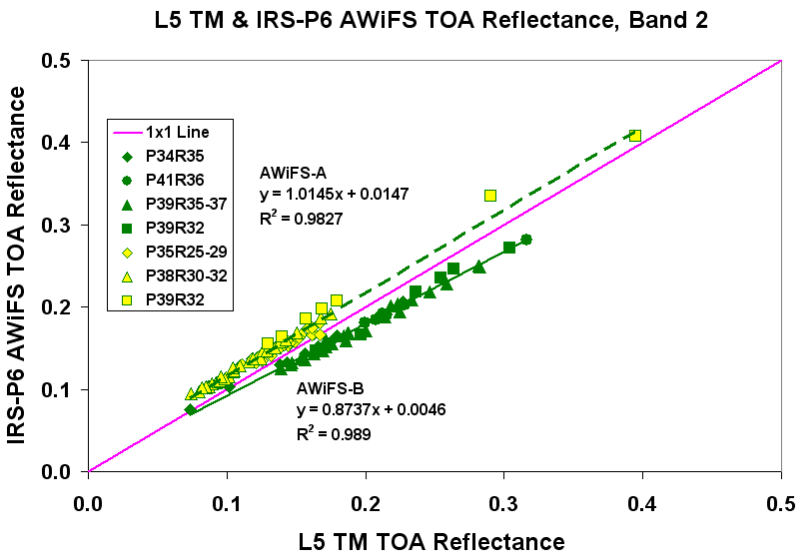

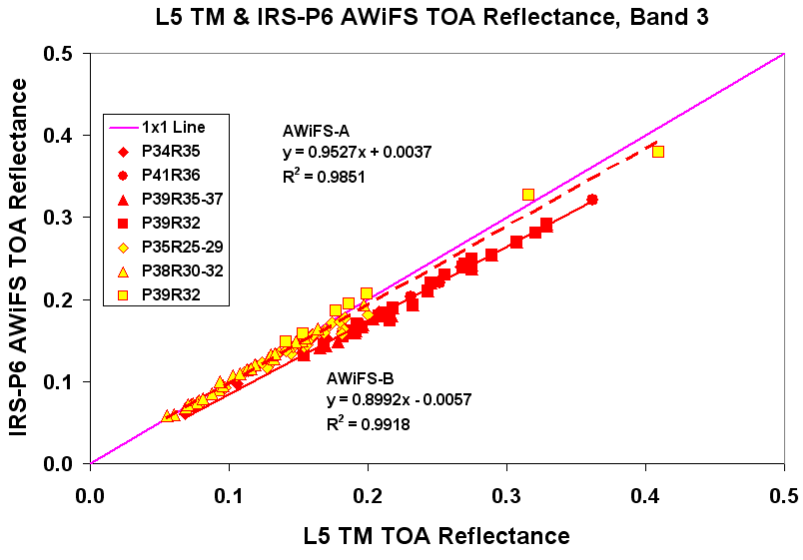

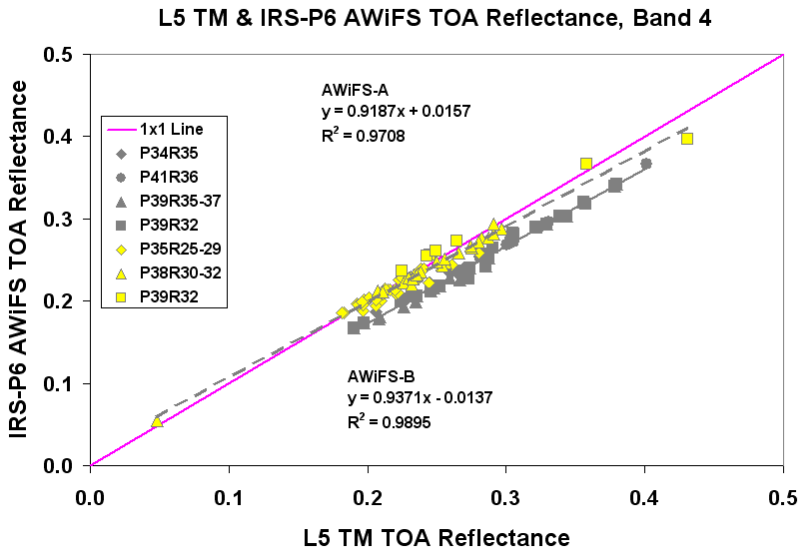

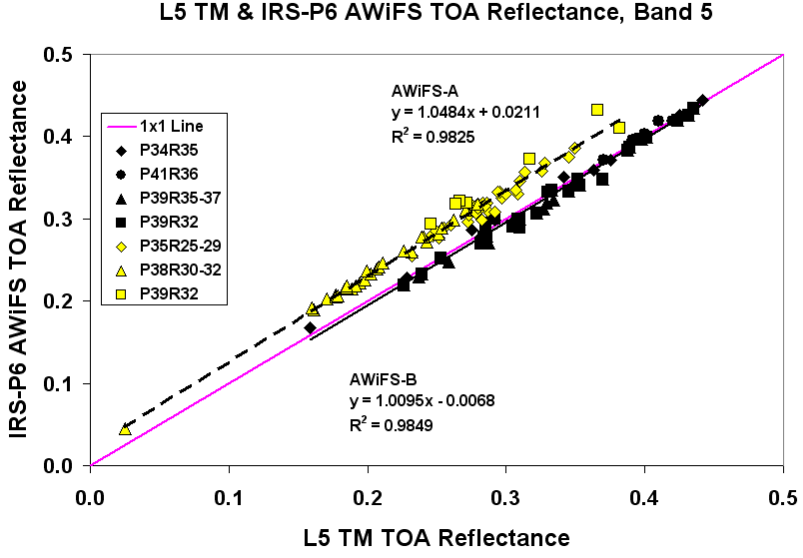

G. Cha

Cross-comparison uncertainty due to the spectral band differences between the sensors

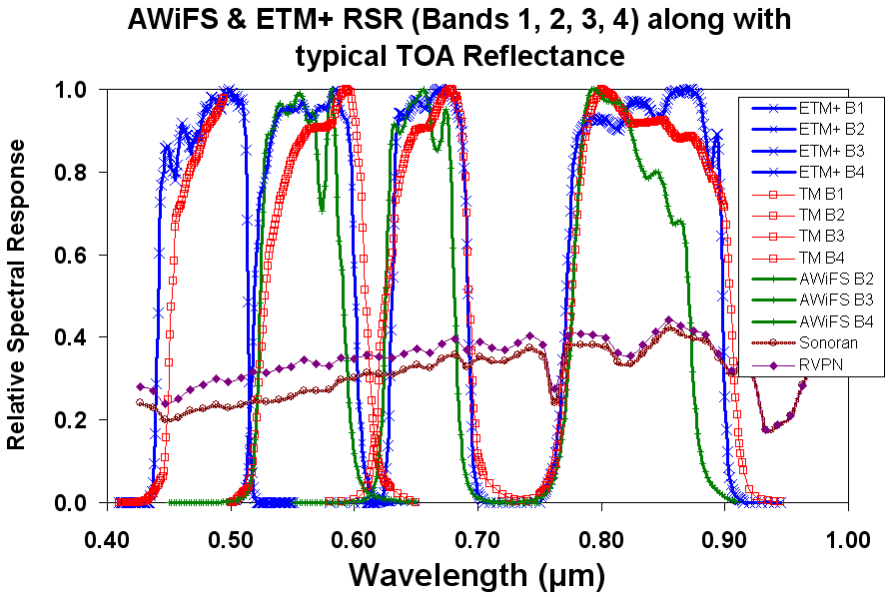

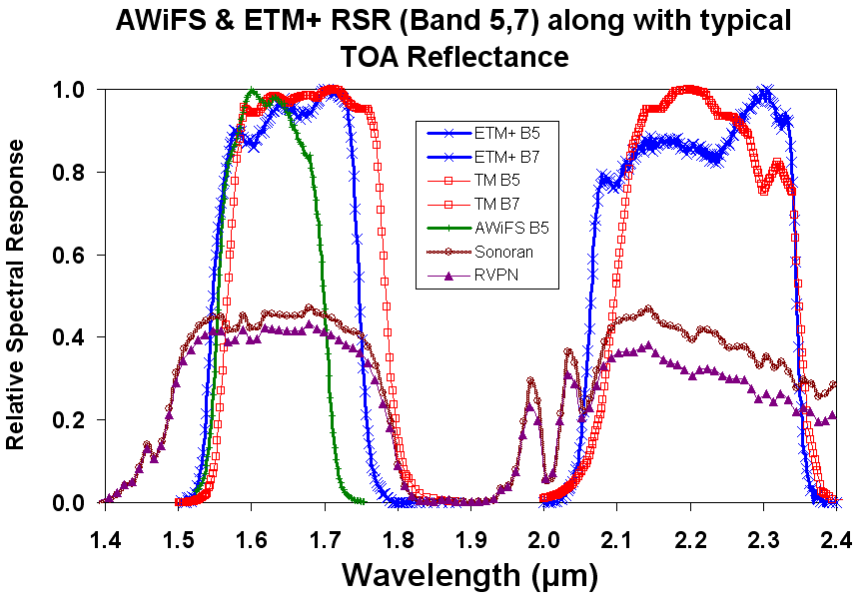

- SBAF were derived using hyperspectral EO-1 Hyperion measurements
- To understand the impact of the sensor spectral response differences on TOA reflectance measurements, the following equations were used

$$SBAF = \frac{\rho_{ETM+}}{\rho_{AWiFS}} = \frac{\left(\int \rho_\lambda \, RSR_{\lambda(ETM+)} d\lambda\right) \Big/ \left(\int RSR_{\lambda(ETM+)} d\lambda\right)}{\left(\int \rho_\lambda \, RSR_{\lambda(AWiFS)} d\lambda\right) \Big/ \left(\int RSR_{\lambda(AWiFS)} d\lambda\right)}$$

SBAF over RVPN (AWiFS)		
Bands	L7 ETM+	L5 TM
2	1.004	1.016
3	1.008	1.005
4	0.992	0.984
5	0.982	0.928

SBAF over Sonoran (AWiFS)		
Bands	L7 ETM+	L5 TM
2	0.972	1.054
3	0.940	1.006
4	0.985	0.987
5	0.986	0.933

G. Chander (gchander@usgs.gov) JACIE Workshop

Cross-comparison uncertainty due to mis-registration between the sensors

To check the sensitivity of the regions to image geometry, a moving window technique was used

The selected ROI (100x100 pixels) were shifted by few pixels (1, 2, 3, 4, 5, 10, 15, 20, 25 Pixels) in horizontally right and left and vertically up and down

Absolute % difference (APD) for each ROI (r) and scene (s)

$$APD_{sr} = \left(\frac{|\mu_{sr} - \mu_{sr'}|}{\mu_{sr}} * 100 \right)$$

$$APD_s = mean(APD_{sr})$$

$$APD = mean(APD_s)$$

RVPN (P40R33)
Sonora (P38R38)
Range Land (P35R30)
Grass Land (P31R31)
Deciduous Forest (P14R31)
Coniferous Forest (P46R30)

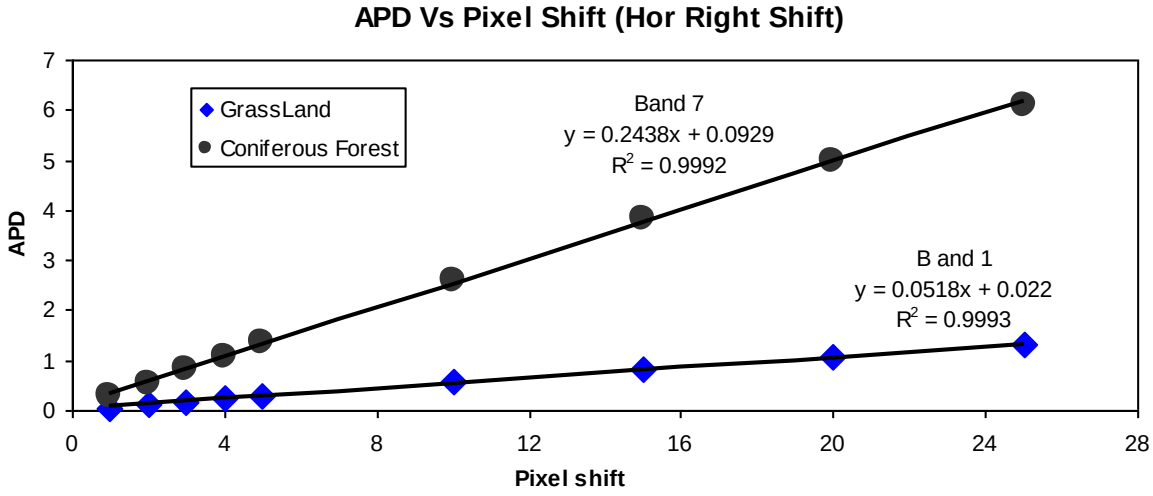

G. Chander (gchander@usgs.gov) JACIE Workshop

Long-term TOA Reflectance Trending (Sonoran & Railroad Valley Test Sites)

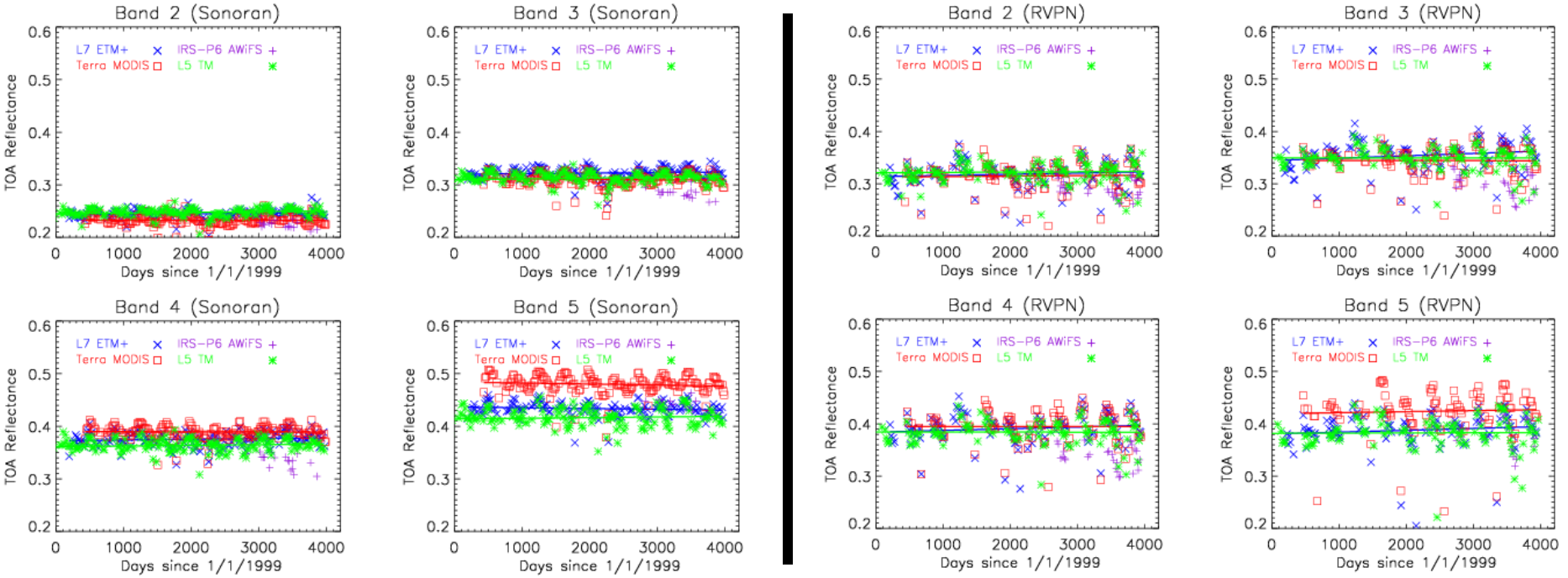

- Linear equations are fitted to the long-term TOA reflectance trends
  - Slope values are very small: prove the long term stability of sensors
  - There are constant offsets: caused by a combination of the spectral signature of the ground target, atmospheric composition and the RSR characteristics
- The annual oscillation were caused by BRDF effect

Long-term TOA Reflectance Trending (Sonoran & Railroad Valley Test Sites)

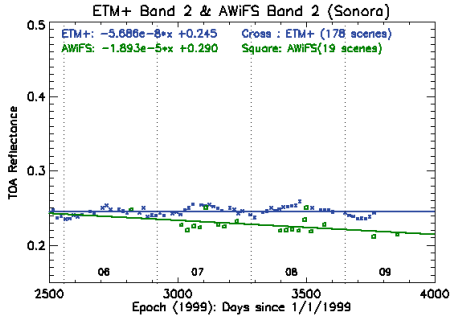

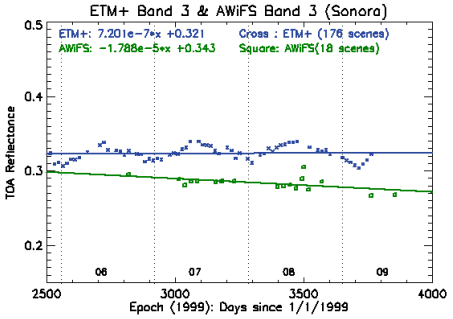

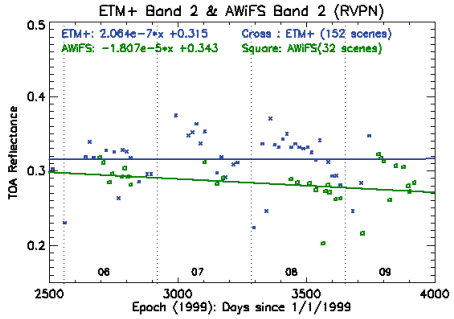

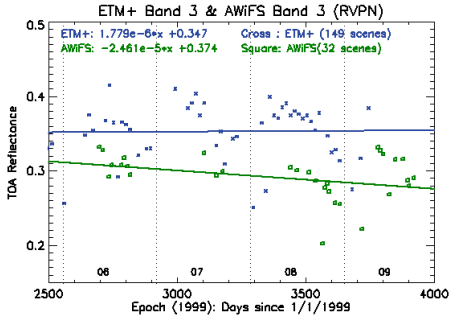

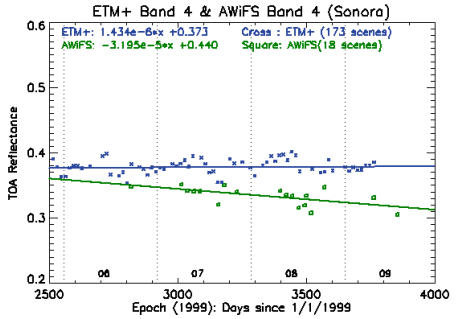

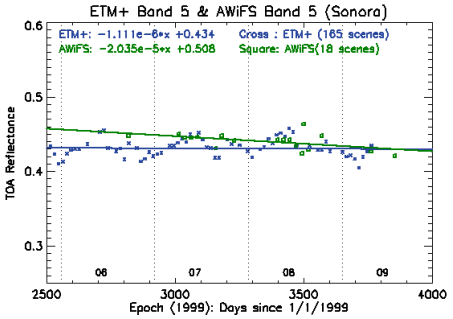

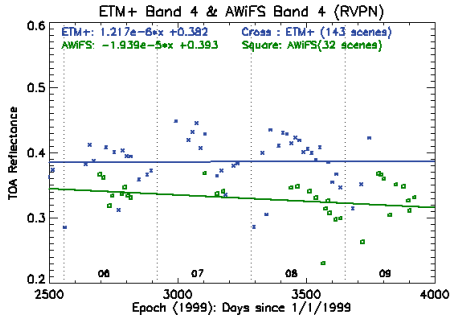

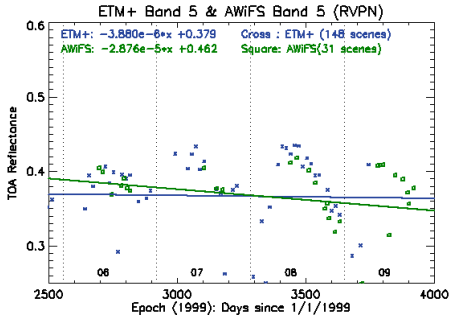

AWiFS				
Band	**Slope**	**t-value**	**p value**	**Ho, slope=0**
Sonora				
2	-1.900E-05	-2.1	0.0505	Fail to reject
3	-1.788E-05	-2.58	0.0203	Reject
4	-3.200E-05	-3.15	0.0062	Reject
5	-2.035E-05	-2.42	0.0279	Reject

Image-to-Image (I2I) Assessment (Sonoran & Railroad Valley Test Sites)

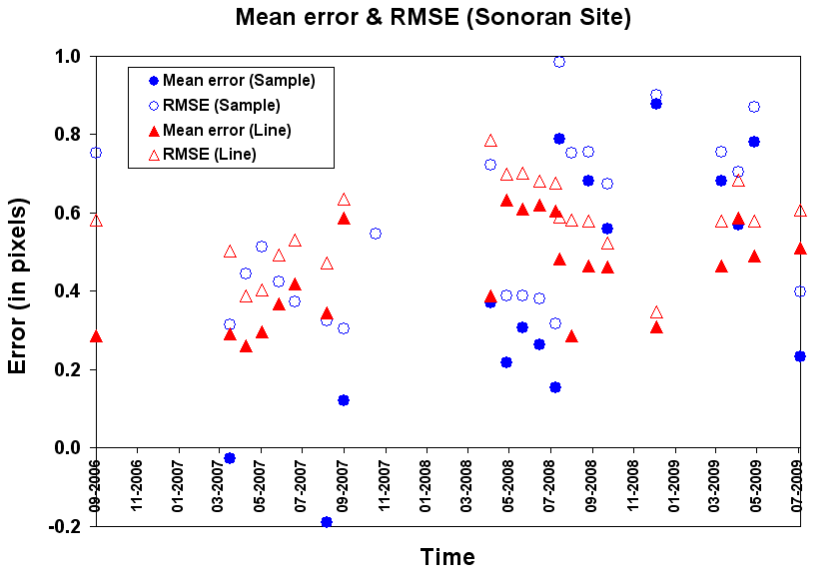

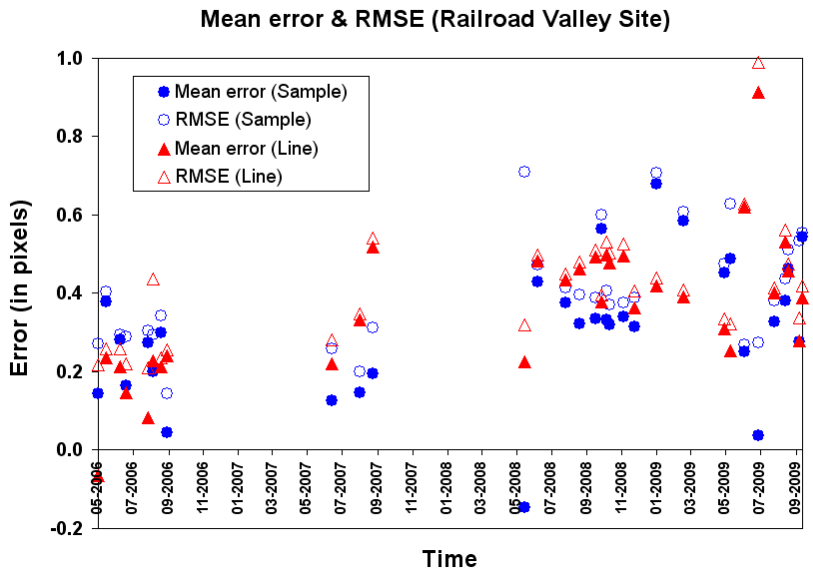

- The I2I characterization was performed to compare the relative accuracy between two images
  - One image is selected as a reference and another as the search image
  - A total of 33 AWiFS images over Railroad Valley, and 22 images over Sonoran were compared against the GLS2000 dataset
  - The AWiFS images were typically registered to within one pixel to the GLS2000 dataset
- The RMSE measured between the AWiFS image and the reference ranged from 11.78 to 55.44 m (0.21–0.99 pixel) in the line direction and from 8.02 to 39.79 m (0.14–0.71 pixel) in the sample direction for the RVPN dataset

Science Assessment

- The goal of this study, is the evaluate the suitability of P6 AWiFS sensors for LCLUC applications through a comparison with legacy data sets generated from Landsat data

- Monitoring Trends in Burn Severity (MTBS)
- Multi-Resolution Land Characteristics Consortium (MRLC)
- LANDFIRE

G. Chander (gchander@usgs.gov) JACIE Workshop

Monitoring Trends in Burn Severity: MTBS

- Mapping the Location, Extent and Severity of Fires in the United States
- Burn severity products are based on the differenced Normalized Burn Ratio (dNBR) derived from Landsat TM & ETM+ data:
- Normalize Burn Ratio (NBR) = (B4 – B7) / (B4 + B7)
- dNBR = PreFire NBR – PostFire NBR
- Burn Severity is visually estimated from the dNBR

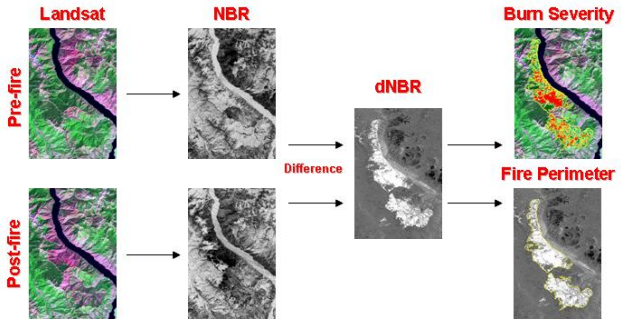

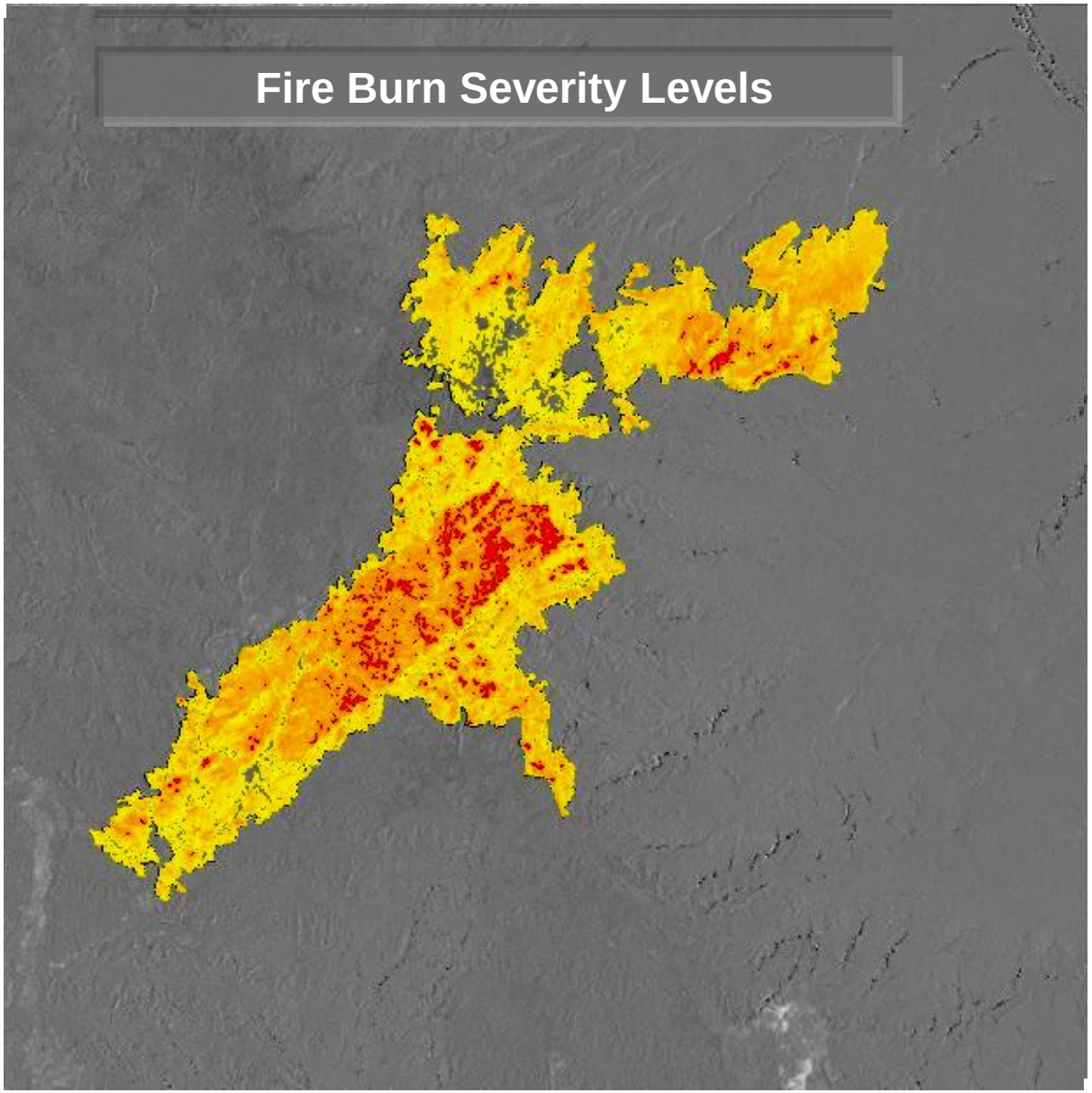

G. Chander (gchander@usgs.gov) JACIE Workshop

MTBS Burn Severity Maps Assessment
Data Sources

Arizona Warm Fire
(July 06, 2006)

Mostly Ponderosa pine with a Pinyon Juniper/ Shrub mixture at lower elevations on the east

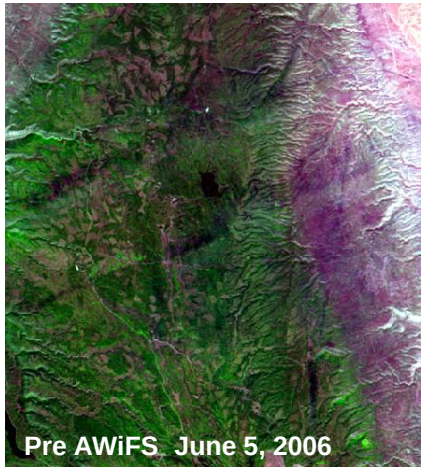

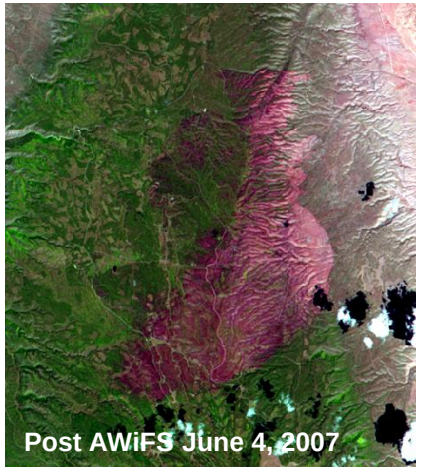

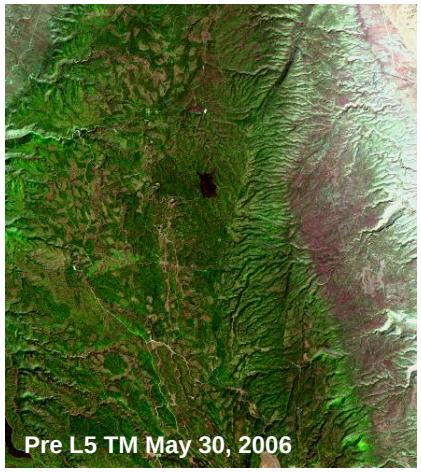

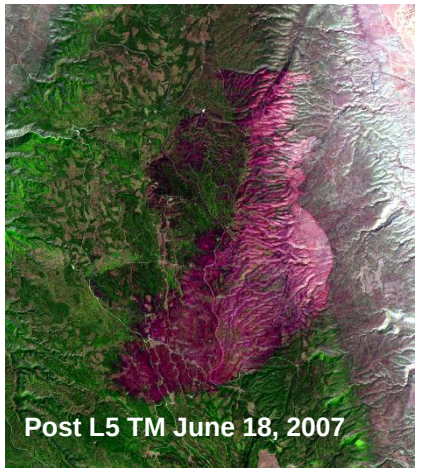

Pacific NW Columbia Complex Fire
(Aug 21, 2006)

Primarily in evergreen forest but also in surrounding agricultural lands and adjacent to a previous burn

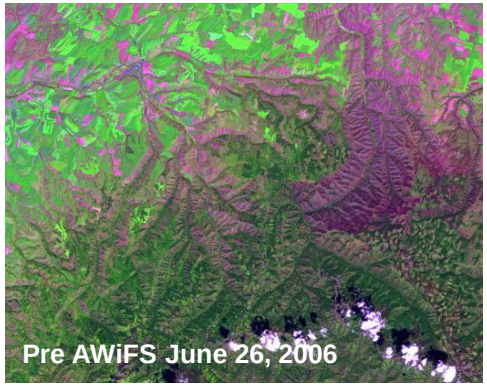

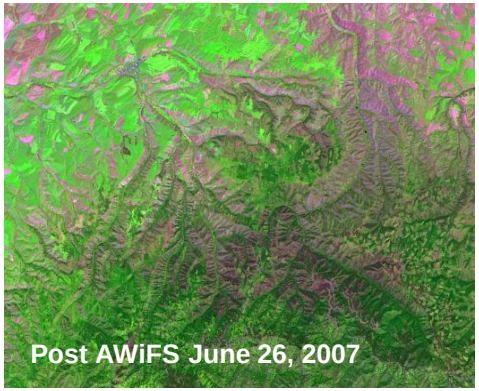

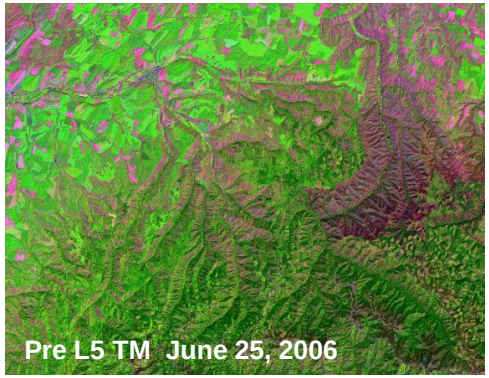

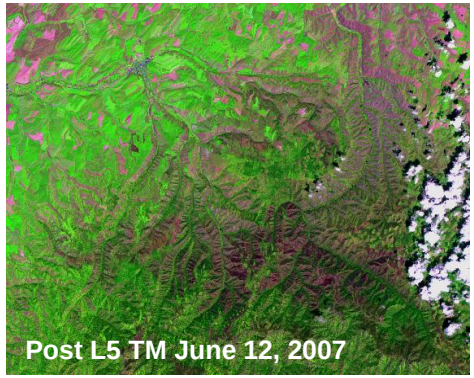

G. Chander (gchander@usgs.gov) JACIE Workshop

MTBS dNBR Burn Severity Maps:

Arizona, Warm Fire [July 06, 2006]

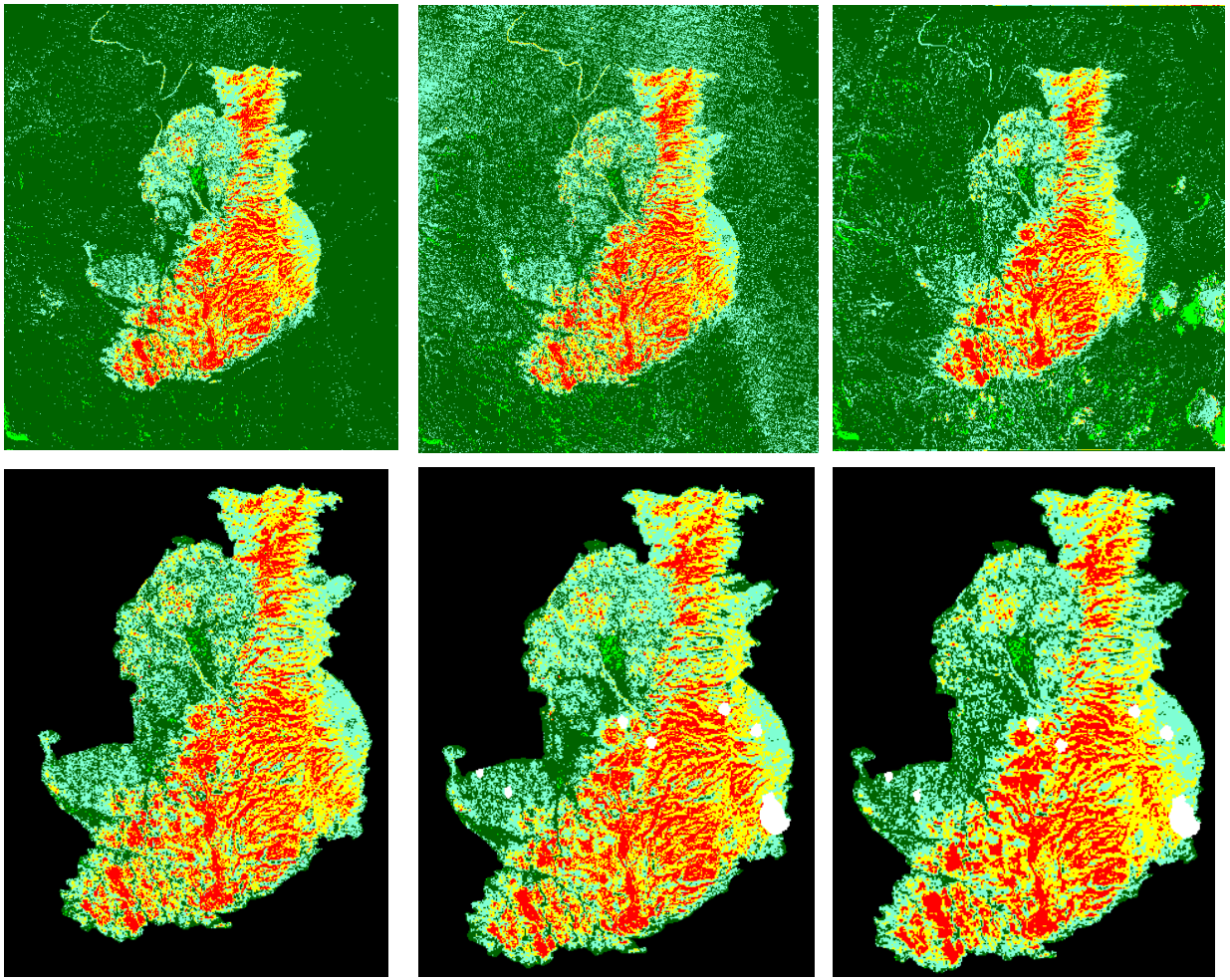

Official TM dNBR | TM B5 dNBR | AWiFS dNBR

Visually all the maps look very similar

In the TM B5 map, the confusion between the unburned and low severity class outside the perimeter is because of using B5 which is not as sensitive as B7

In the AWiFS map, the confusion is reduced because of the coarser spatial resolution of 56 m that may cause a smoothing effect

Table shows a comparison of "official TM" versus "AWiFS" dNBR

Class Severity	Pixel Counts	Class 1	Class 2	Class 3	Class 4	Total	% agreement
Unburned to low	Class 1	9713	4301	59	1	14223	68.3
Low	Class 2	4224	17114	3098	40	24479	69.9
Moderate	Class 3	14	3318	15478	2781	21591	71.7
High	Class 4	0	16	2815	11535	14366	79.6

MTBS dNBR Burn Severity Maps:
Pacific NW Columbia Fire [Aug 21, 2006]

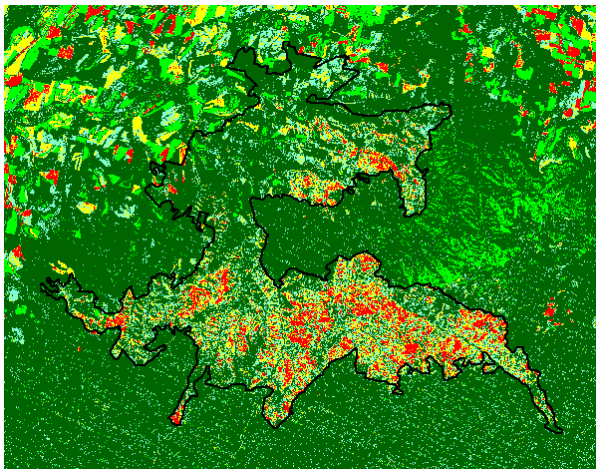
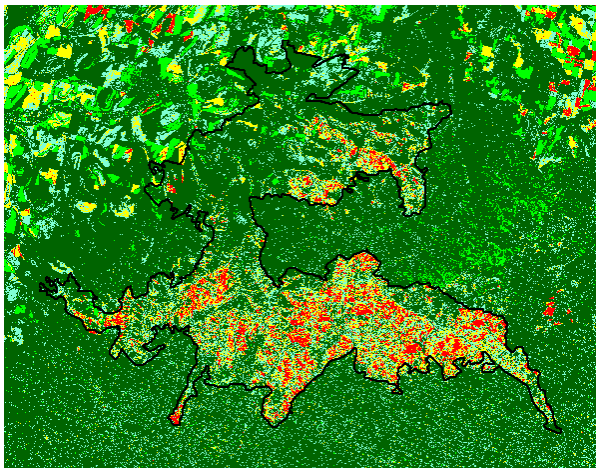
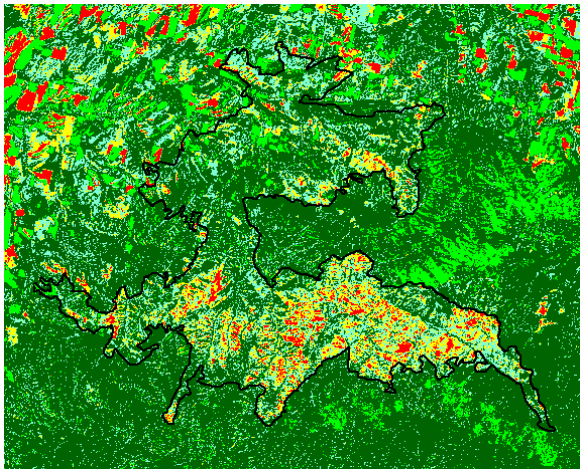
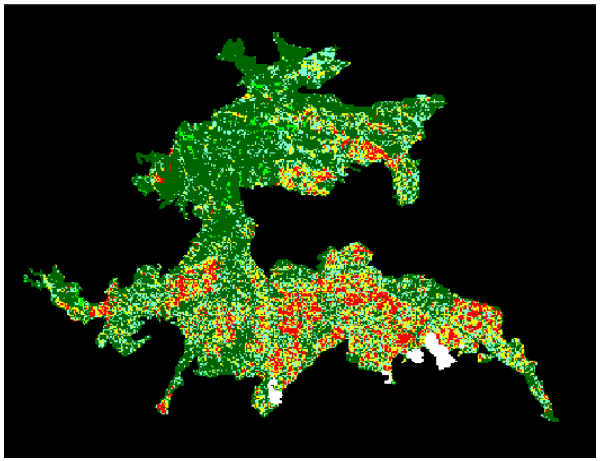
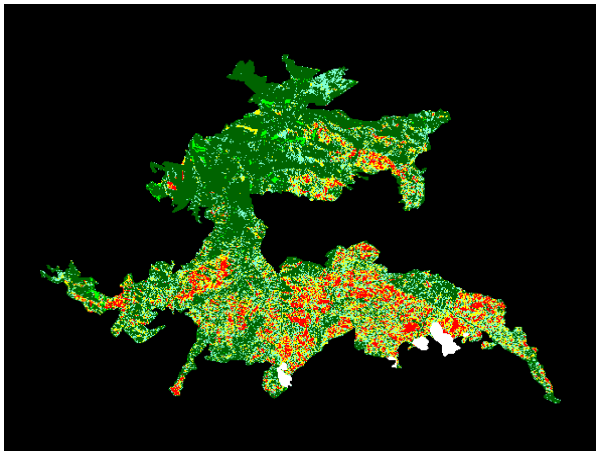
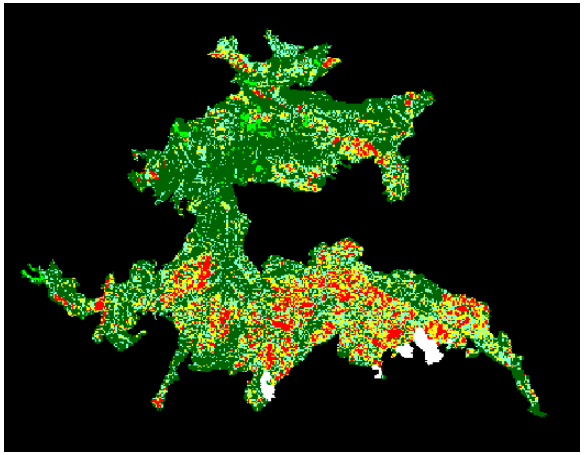

Official TM dNBR | **TM B5 dNBR** | **AWiFS dNBR**

Class Severity	Pixel Counts	Class 1	Class 2	Class 3	Class 4	Total	% agreement
Unburned to low	Class 1	62997	12866	4102	802	81933	76.9
Low	Class 2	13733	9795	5837	958	30472	32.14
Moderate	Class 3	3919	6437	9287	3598	23277	39.9
High	Class 4	293	1046	4093	10299	15733	65.46

NLCD Tree Canopy Change Assessment

Seattle (Mostly Forest)

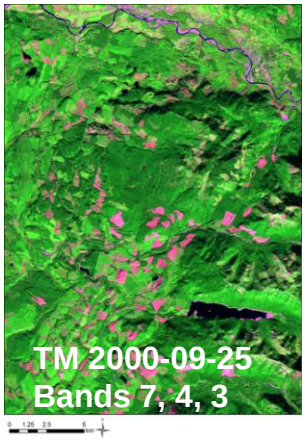

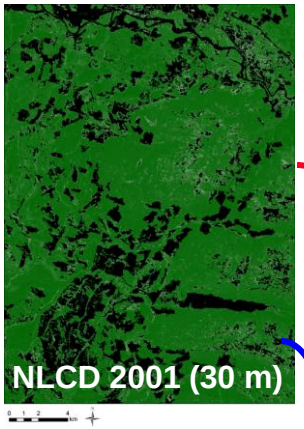

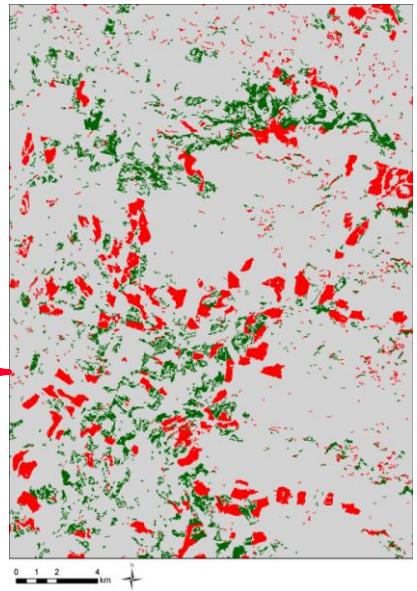

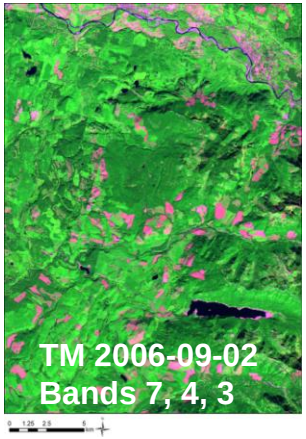

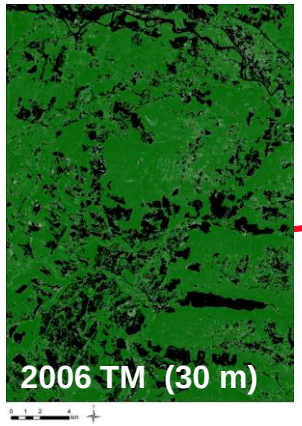

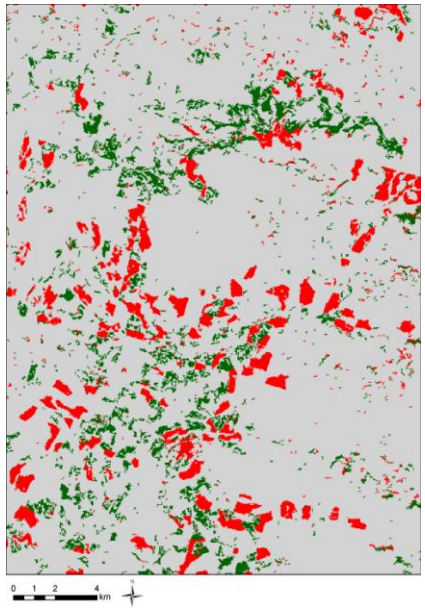

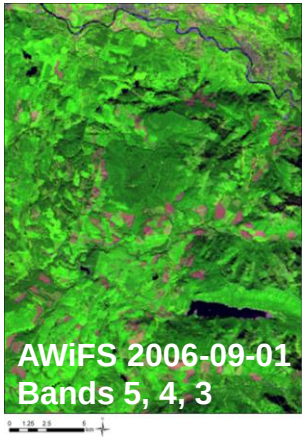

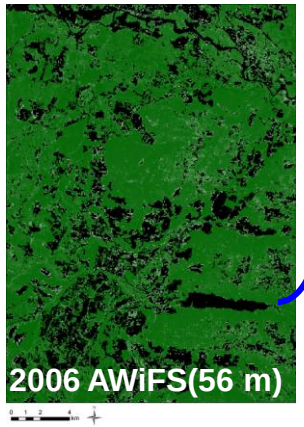

Data

Tree Canopy

Tree Canopy Change

Change comparison for Tree Canopy derived from Landsat and AWiFS Images

Change Agreement	
Seattle	
Decrease area	Increase area
56 m	
87.40%	84%
30 m	
76%	72%

NLCD Tree Canopy Change Assessment

San Diego (Forest, Grassland, Shrubland, etc.)

Decrease in tree canopy estimate is relatively easy to detect (spectral variation due to fire disturbance, clear-cut)

Increase is a gradual change. Increase in tree canopy estimate is harder to detect. (Spectral mixing makes it harder to detect re-growth)

Change comparison for Tree Canopy derived from Landsat and AWiFS Images

Change Agreement	
San Diego	
Decrease area	Increase area
56 m	
82.10%	42%
30 m	
42%	27.40%

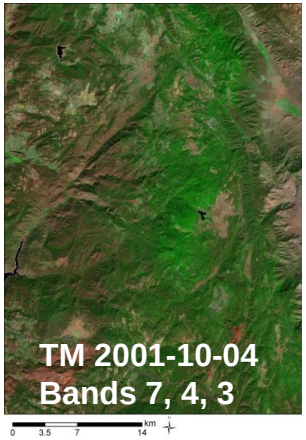

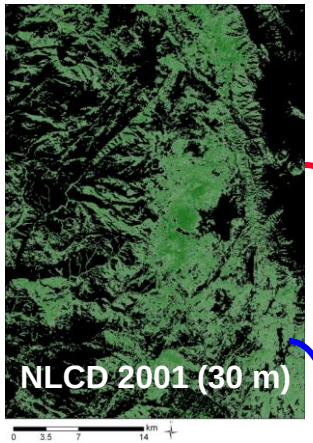

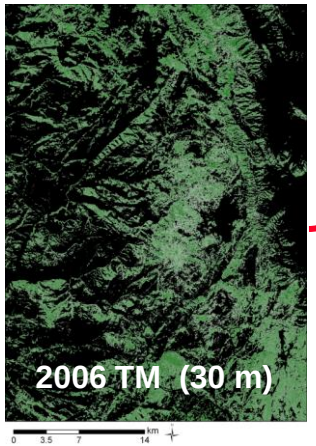

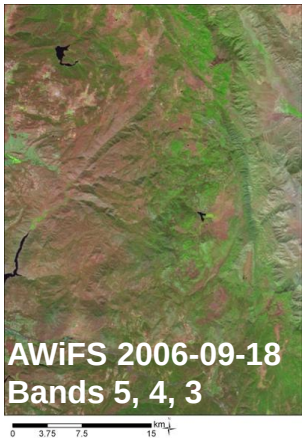

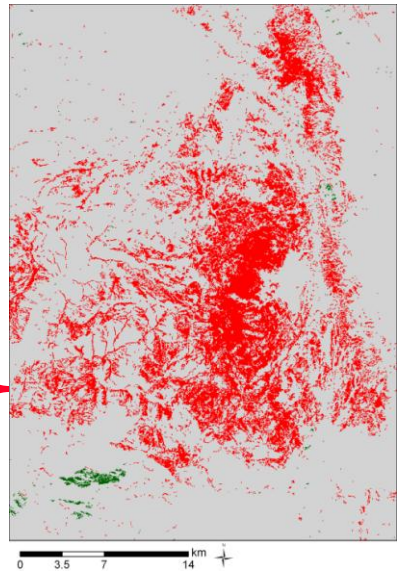

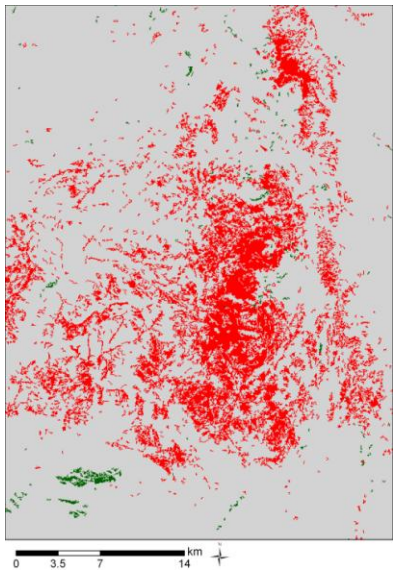

Data

Tree Canopy

Tree Canopy Change

NLCD Wetland Mapping and Monitoring
Data Sources

- Challenges
  - Composition of wetlands is complex and often with mixed components (vegetation species, soil, water, etc.)
  - Condition of wetlands are dynamic (seasonal, interannual)
  - Spatial distribution of wetlands are complex
- Remote Sensing Data
  - QuickBird: Sept 29, 2006
  - Landsat TM: Sept 26, 2006
  - IRS-P6 AWiFS: Sept 27, 2006
- Field data (Wetland type, vegetation, fraction of water, land/soil, etc.)

TM & AWiFS Imagery Footprint
Northern Gulf of Mexico (NGOM) study area
Coastal wetlands in LA, most dynamic environment

G. Chander (gchander@usgs.gov) JACIE Workshop

NLCD Wetland Mapping and Monitoring
Comparison of Modeled Sub-Pixel Percent of Water

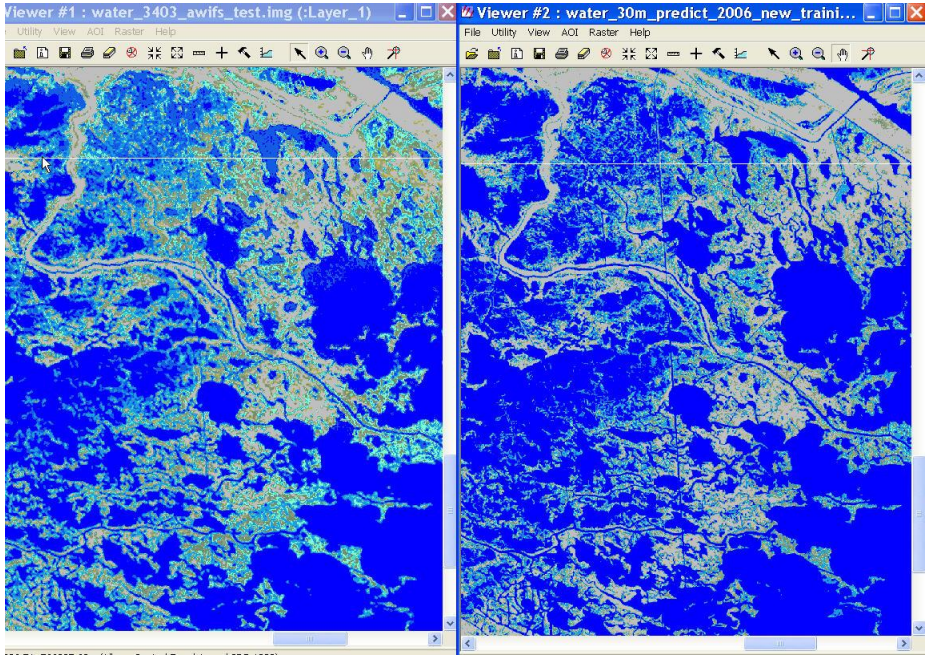

% water Sep. 27, 2006 using AWiFS

% water Sep. 26, 2006 using Landsat

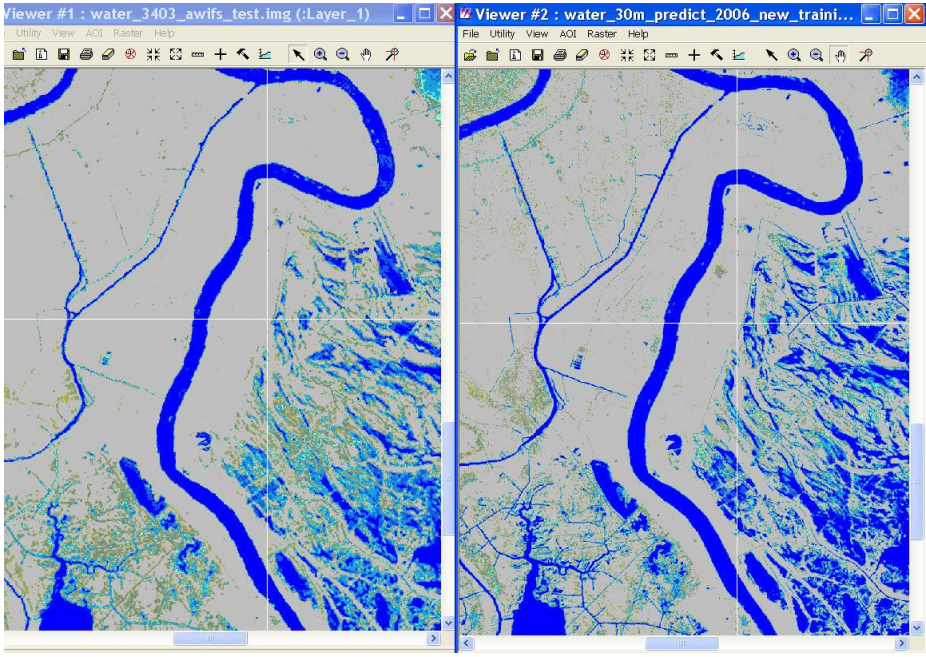

% water Sep. 27, 2006 using AWiFS

% water Sep. 26, 2006 using Landsat

The model prediction used all the Landsat 6 solar reflective bands, while it used 4 AWiFS bands
In general, TM and AWiFS % water estimate pattern are very similar spatially
The coarser spatial resolution of AWiFS (56 m) causes fuzziness in linear features

Input Imagery	# of training samples	# of test samples	Ave Error (%)	Relative Error (%)	Correlation Coeff. R
TM Image	5000	500	6.4	0.15	0.96
AWiFS Image	5000	500	9.8	0.23	0.90

G. Chander (gchander@usgs.gov) JACIE Workshop

Science Utility Evaluation Summary

- Indicates that AWiFS data is potentially a usable alternative to Landsat during the mission gap
  - The higher radiometric resolution (10 bits), larger swath area coverage (740 km), and a frequent repeat cycle (five days) will be an advantage for science applications, allowing for the increased likelihood of cloud-free acquisitions and reduction in the processing and handling of a lower number of images
  - The coarser spatial resolution (56 m) and lack of an AWiFS equivalent to the Landsat spectral Band 1/7 can have an adverse impact on a few assessments, likely resulting in reduced but acceptable derived-product accuracy and sensitivity
  - The coarser spatial resolution of AWiFS could negatively impact the ability to discriminate fine-scale landscape features, especially those related to urban development (It is possible, however, that the disadvantage of lower spatial resolution could be offset by the more frequent repeat coverage of AWiFS)

G. Chander (gchander@usgs.gov) JACIE Workshop

Future Work

- Characterize the uncertainties due to spectral mismatches, spatial, radiometric, BRDF, and atmospheric impacts
- Investigate differences between Camera AC/BD
- Get additional data to track the long term stability of the AWiFS sensor
- Investigate the impact of cross-cal coefficients on LCLUC science applications
- ResoureSat-2 characterization

Contributors

- The slides in this presentation include contributions from a number of individuals in various organizations
  - USDA/FAS (Tetrault)
  - USGS/EROS (Stensaas, Howard, McKinley, Homer, Yang, Xian, Vogelmann, Chen, Tolk, Sampath)
  - NASA/MCST (Xiong, Angal, Choi)
  - SDSU (Helder, Shrestha, Mishra)
  - Others!

- This work was supported by Dr. Gutman through the NASA LCLUC Grant NNH08AI30I